DNA origami

Controlled Delivery of DNA Origami on Patterned Surfaces**

Aren E. Gerdon, Seung Soo Oh, Kuangwen Hsieh, Yonggang Ke, Hao Yan, and H. Tom Soh**

Due to its capacity for programmable self-assembly, well-established modes of chemical synthesis, and exceptional stability, DNA serves as a powerful nanoscale structural material.[1,2] In particular, the recent invention of DNA origami technology[3] has established a paradigm in which DNA's capacity for deterministic self-assembly into essentially any discrete two-dimensional (2D) shape can be exploited for the construction of molecular ''bread boards''. For example, previous groups have demonstrated the delivery of nanoparticles to specific positions within an origami scaffold with nanometer-scale precision[4] and the weaving of DNA aptamers[5,6] into origami for the assembly of protein arrays.[7] However, in order to fully harness the potential of DNA as a universal nanoscale template, it is important not only to control the position of cargo material within the origami scaffold but also to accurately control the position and orientation of the origami itself with respect to other features on a wafer. Although some progress has been reported,[8,9] this has proven to be a significant challenge, and an effective universal approach is critically needed.

To this end, we report a strategy that combines top-down fabrication and bottom-up self-assembly to achieve deterministic position control of DNA origami structures over millimeter length scales on a wafer. To achieve this goal, we formulated a chemical strategy to attract and immobilize the origami onto gold surfaces using a carboxylic acid-terminated self-assembled monolayer (SAM). Furthermore, we have developed a technique for performing atomic force microscopy (AFM) on gold, rather than mica, surfaces in order to image these origami structures. Using these methods, we demonstrate 1) selective immobilization of DNA origami onto gold surfaces and 2) controlled delivery of a single DNA origami scaffold onto a single nanometer-scale gold pattern. Furthermore, we show that the pre-positioned origami can be utilized as a template such that gold nanoparticles can be accurately positioned within the structure. Two rectangular origami designs with dimensions of $90 \times 60 \times 2$ nm^3 ($L \times W \times H$) were constructed using M13 phage DNA and 226 short DNA staple strands[7] (Figure 1). Design B is identical to Design A except that it incorporates 12 extra strands of DNA consisting of 12 consecutive thymine residues (T_{12}), which are clearly visible via AFM. To confirm the yield of the origami assembly, these designs were cast onto freshly cleaved mica and imaged using tapping-mode AFM in liquid. The rectangular features of the origami were clearly visible in both height and phase modes, and we observed nearly 100% of assembly yield, as previously reported[10] (Figure 2A). In phase mode,[11,12] the origami structures appear as dark rectangles — consistent with previous observations of DNA structures on mica[13,14] (Figure 2A, column 3).

Previously, high-resolution AFM of DNA origami has been performed almost exclusively on mica surfaces due to its atomic-level flatness, and imaging on gold surfaces has not been previously reported, due to the challenges arising from significant surface roughness. To overcome this problem, here we developed a process to produce flat gold surfaces on silicon wafers. First, we deposited a 2-μm-thick gold layer on a 200-nm-thick titanium sticking layer on a silicon wafer using electron-beam physical evaporation. Subsequently the wafer was mechanically polished using 0.02-μm colloidal silica and thermally annealed at 300 °C for 3 h in air. This process resulted

[*] Prof. H. T. Soh, S. S. Oh[+]
Materials Department
University of California
Santa Barbara, CA 93106–5070 (USA)
E-mail: tsoh@engr.ucsb.edu
Prof. H. T. Soh, K. Hsieh
Department of Mechanical Engineering
University of California
Santa Barbara, CA 93106–5070 (USA)
Prof. H. Yan, Y. Ke
Department of Chemistry and Biochemistry
and the Biodesign Institute
Arizona State University
Tempe, AZ 85287 (USA)
E-mail: hao.yan@asu.edu
Prof. A. E. Gerdon[+]
Department of Physics and Chemistry
Emmanuel College
Boston, MA 02115 (USA)
[+] These authors contributed equally to this work.

[**] A.E.G. thanks Jonas Perez of Vanderbilt University for helpful discussions on nanoparticle functionalization, and Bill Mitchell of UCSB Nanofabrication Facility for his assistance in electron beam lithography. H.T.S. is grateful for financial support from ONR, NIH, and ARO Institute for Collaborative Biotechnologies (DAAD1903D004). H.Y. thanks the funding support of NSF, ONR, AOR, AFOSR, and NIH. All nanofabrication was carried out at the NSF-supported Nanofabrication Facility at UC Santa Barbara.

DOI: 10.1002/smll.200900442

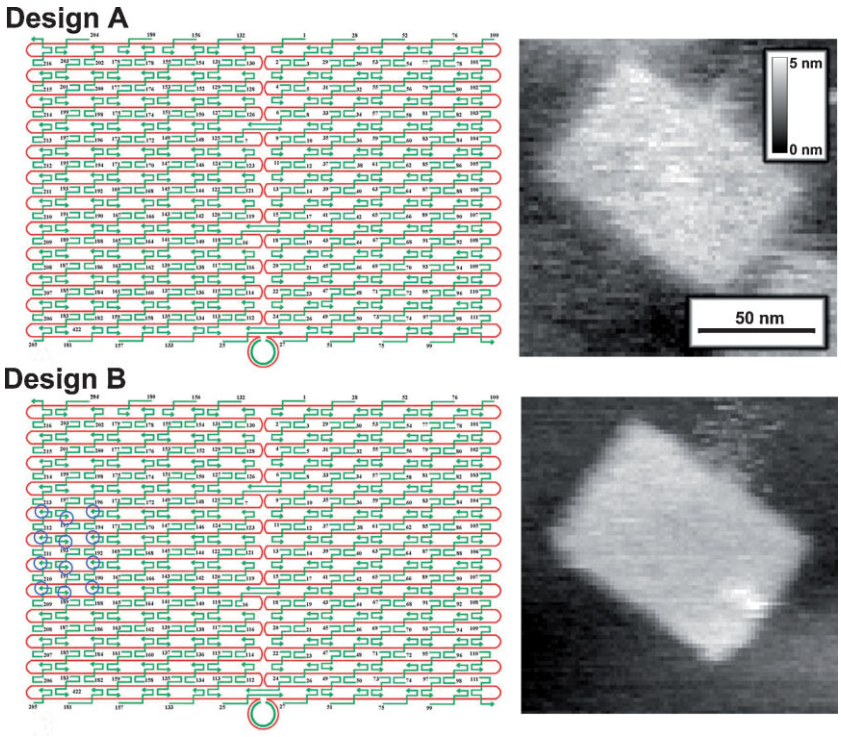

Figure 1. Design diagrams and AFM micrographs of the two origami structures (note: both AFM images are taken at the same scale). Design A consists of a single, continuous M13 phage DNA (red) and 226 short helper strands (green). The helper strands co-operatively bind to the M13 DNA to form the origami. The rectangular shape is clearly visible in AFM micrographs. Design B is identical to Design A, with the exception that it contains 12 additional strands of T_{12} segments that protrude from the plane of the origami (blue). The protrusions can be observed in the AFM image.

in a smooth gold surface with RMS roughness of 0.6 nm (data not shown). Next, in order to attract and immobilize the origami, the gold surface was functionalized with 11-mercaptoundecanoic acid (MUA),[15] a carboxylic acid-terminated SAM. The carboxylic acid groups concentrate and chelate magnesium ions in the buffer at the gold surface, thereby promoting a strong ionic attraction between the negatively charged origami and the positively charged magnesium, creating an effective salt bridge to the gold surface.[16,17] Using this approach, we obtained clear AFM images in both height- and phase-imaging modes on gold surfaces (Figure 2B, columns 2 and 3). Next, we confirmed that the formation of these magnesium salt bridges is essential for origami immobilization, and found that when we functionalized the gold surface with 6-mercaptohexanol (MH), a hydroxyl-terminated SAM that does not chelate Mg^{2+}, we did not observe any origami scaffolds using either imaging mode (Figure 2C). AFM revealed that the roughness of MUA surface (rms roughness ≈0.553 nm) was less that of the MH surface (rms roughness ≈0.854 nm).

Using this chemical strategy, we investigated the specificity of DNA origami delivery onto gold surfaces. Due to the fact that gold surfaces are functionalized with MUA, but SiO_2 surfaces are not, magnesium salt bridges can only form on the gold patterns. AFM micrographs revealed no DNA adsorption on SiO_2 surfaces (Figure 3, inset A), whereas origami structures were clearly visible on the gold surfaces (Figure 3, inset B). The highly specific nature of the origami immobilization is most readily apparent at the interface between SiO_2 and gold surfaces (Figure 3, inset C).

Next, we investigated the feasibility of delivering a single origami structure to a single nanofabricated gold pattern using this strategy. An array of gold patterns was prepared with the lift-off process via electron-beam evaporation of titanium/gold (3 nm/3 nm). Each gold dot was ≈70 nm in diameter, which is smaller than the origami, to ensure that only a single origami is delivered. In height mode, AFM micrographs revealed a topography of ≈6 nm for gold features (Figure 4A, columns 2 and 3), and as expected, minimal contrast was observed between the MUA-functionalized gold patterns and the SiO_2 layer in phase mode (Figure 4A, column 4).[18] Next, 5 μL of origami scaffolds (10 nM) were cast onto the wafer, and the resulting AFM micrographs revealed a ≈2-nm increase in the topography (Figure 4B, columns 2 and 3), consistent with the added thickness of the origami, while phase images showed clear contrast due to the large differences in material properties (Figure 4B, column 4). In order to verify the positions of the origami structures with respect to the gold pads, we added 5 μL of 10-nm-diameter gold nanoparticles (2 nM) functionalized with thiolated DNA strands containing 12 consecutive adenosine residues (A_{12}).[19] The T_{12} DNA strands protruding from the origami surfaces (Figure 1, Design B) hybridized to the A_{12} sequences on the nanoparticles, yielding clear contrast and position information. To avoid any non-specific physisorption of the gold nanoparticles, the substrate was stringently washed using 1× TAE buffer, and control experiments revealed no gold nanoparticles after the wash (data not shown).

AFM in both height and phase modes clearly confirmed the delivery of gold nanoparticles onto individual origami rectangles on gold patterns (Figure 4C, columns 2 and 4). The height profile of the labeled patterns (Figure 4C, column 3) revealed the combined height of the origami and gold nanoparticles to be approximately 18 nm, which is consistent with our estimations. Not all immobilized origami rectangles were associated with gold nanoparticles, and we attribute this to the fact that the T_{12} strands are located only on one side of the rectangle; thus, if the origami structure is immobilized with the T_{12} strands facing the gold pattern, this would prevent hybridization with the A_{12} strands on the gold nanoparticles.

In conclusion, we demonstrate the integration of top-down fabrication and bottom-up molecular assembly to position DNA origami structures onto specific locations on a wafer, and delivering nanoparticles to specific locations within those origami scaffolds. The method exploits fundamental processes of magnesium chelation and base-pair hybridization, which is scalable, robust, and reproducible, and could be expanded for

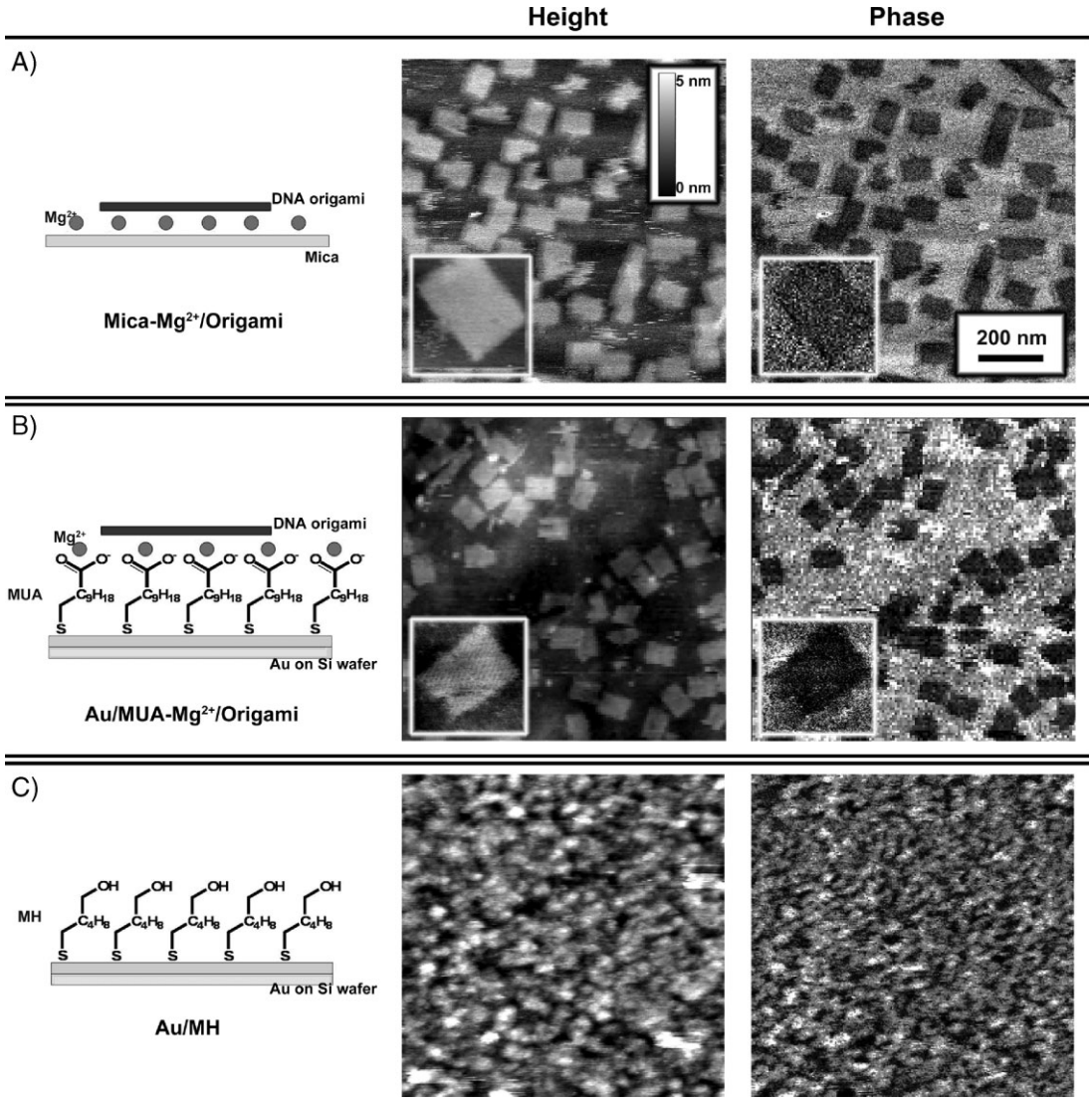

Figure 2. AFM microscopy of DNA origami on mica and gold surfaces. (note: all images are taken at the same scale). A) The formation of magnesium salt bridges between the origami allows efficient immobilization on mica surfaces. The rectangular origami shapes are clearly visible in both height and phase modes. B) Functionalization of gold surfaces with a carboxylic acid-terminated self-assembled monolayer (MUA) enables magnesium chelation and efficient origami immobilization. C) Gold surfaces functionalized with a hydroxyl-terminated self-assembled monolayer (MH) do not display immobilized origami structures.

the controlled delivery of other materials beyond those shown here. Although challenges still lie ahead in controlling the orientation of the origamis, we believe that programmably controlling the position of nanoscale materials with nanometer-scale precision may hold the key to unlocking the full potential of DNA as a structural template material for ultrahigh-density electronic, photonic, and biotechnological applications.

Experimental Section

Materials: Origami strand sequences were based off of a previously reported design [7]. M13 viral DNA was purchased from New England Biolabs, Inc (Ipswich, MA) and DNA helper strands were synthesized by Integrated DNA Technologies (Coralville, IA). All unmodified helper strands and helper strands with additional T_{12} sequences were purchased in 96-well plate format at 25 nm synthesis scale with standard desalting and used as received. Thiolated A_{12} DNA strands (5′-ThioMC6-D/AAAAAAAAAAAA-3′) were synthesized on a 100 nm scale with HPLC purification and also used as received. Millipore Centrifugal Concentrators, 0.5 mL, 100 000 MWCO were purchased from Fisher Scientific (Pittsburgh, PA). Gold colloid (10 nm diameter) and mica discs were purchased from Ted Pella, Inc. (Redding, CA). Olympus Biolever AFM tips were purchased from Asylum Research (Santa Barbara, CA). 11-mercaptoundecanoic acid (MUA) was purchased from Sigma (St. Louis, MO). All reagents were prepared and handled according to supplier specifications, buffers were prepared according to standard laboratory procedures, and all other chemicals were reagent grade and used as received.

Assembly of DNA origami: To assemble DNA origami, helper strands were pooled together to make a master mix, with different

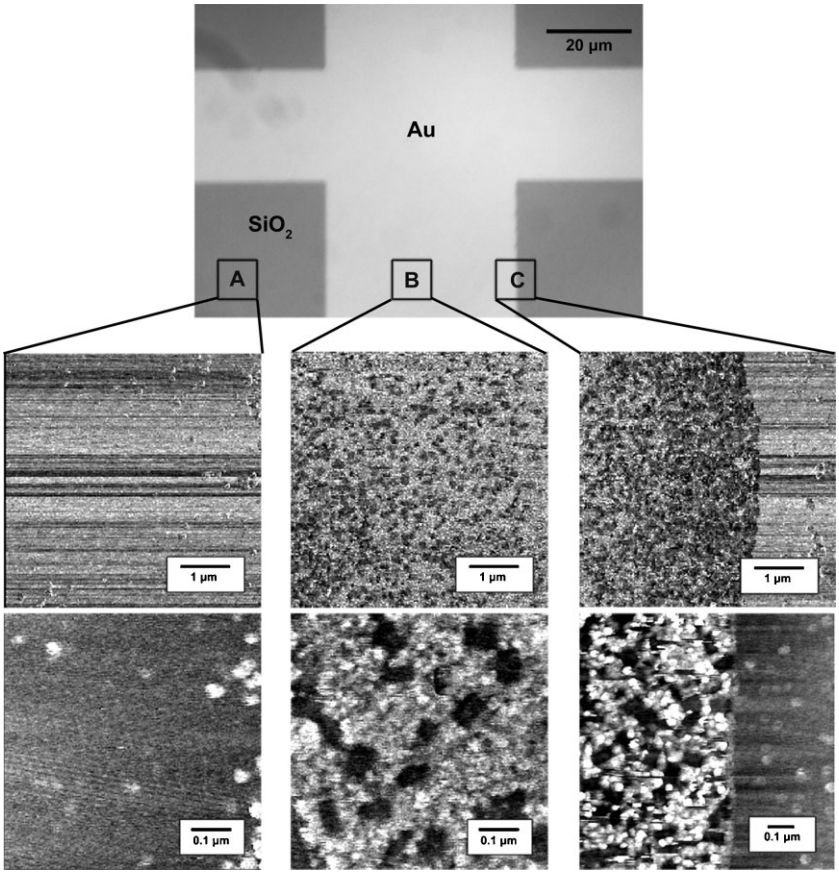

Figure 3. Optical micrograph of a test structure used to demonstrate the selective delivery of DNA origami structures on gold surfaces. Inset A) Phase-mode AFM micrograph reveals that origami structures do not immobilize on SiO_2 surfaces due to the lack of magnesium salt bridges. Inset B) Origami structures are efficiently immobilized on MUA-functionalized gold surfaces. Inset C) The distribution of origami structures at the interface between gold and SiO_2 illustrates the specificity of delivery.

mixes prepared for the different combinations or positions of additional T_{12} strands. After mixing equal amounts of helper strands, the final concentration of each strand in the master mix was 442 nM. Helper strands were then mixed with M13 DNA, TAE buffer, and DI water to a final volume of 100 μL, with final concentrations of 10 nM M13, 30 nM helper strands, 40 mM Tris-HCl, 20 mM sodium acetate, 2 mM EDTA, and 12.5 mM Mg^{2+} (1× TAE buffer). The sample was then heated to 94 °C in a thermal cycler (Bio-Rad, Hercules, CA) and cooled in the following stages: 94 °C to 70 °C (2 °C/5 min), 70 °C to 40 °C (2°/10 min), 40 °C to 25 °C (2 °C/5 min). The resulting origami mixture was stable for several weeks when stored at 4 °C. See origami designs in Figure 1.

Origami Purification: Extraneous helper strands were removed, when necessary, using 100000 MWCO centrifuge filters. To purify, 100 μL of fresh origami mixture was combined with 100 μL of TAE buffer and centrifuged at 2000 rpm for 7–8 min. The liquid was then removed from the bottom of the centrifuge tube and an additional 100 μL of TAE buffer was added to the filter. This was repeated three times and the final purified origami was removed from the top of the filter. Purified origami structures were stable for several days at 4 °C.

Nanoparticle Preparation: Gold colloid was functionalized with thiolated A_{12} DNA in order to hybridize with T_{12} strands on the origami structures. A_{12} DNA was first reduced in 5 mM TCEP for 10 min. Nanoparticles (2.9×10^{12} particles, $\approx 5 \times 10^{-12}$ moles) were then added to 1.2×10^{-9} moles of thiolated A_{12} DNA and reacted for 30 min. Phosphate buffered saline (PBS) was then added to yield a final concentration of 10 mM phosphate, 125 mM NaCl, 2.5 mM KCl, and 0.02% tween-20 and reacted for 1 h. Additional NaCl was then added to a final concentration of 205 mM NaCl and reacted for 1 h, then added again to a final concentration of 285 mM and reacted for an additional hour. The nanoparticle/DNA conjugates were then centrifuged at 13200 rpm for 40 min, the supernatant removed, and fresh PBS added. This was repeated several times and the nanoparticles were ultimately diluted to a concentration of 2 nM and stored at 4 °C.

Surface Fabrication: First, unpatterned gold surfaces were mechanically polished using a polishing machine (Multiprep system, Allied High Tech Products, INC) with 0.02-μm colloidal silica. The gold surfaces were annealed at 300 °C for 3 h to improve their smoothness. The treated gold surfaces had a root mean square (RMS) roughness value of less than 0.6 nm. Micrometer-sized gold patterns were fabricated using an electron-beam evaporator (Temescal/Airco 1800). Titanium (1 nm) and gold (2 nm) were deposited on the <100> silicon wafer with the slow deposition rate (≈0.2 nm/s). The fabricated micrometer-sized gold patterns had RMS roughness of ≈1.5 nm. For nanofabricated gold patterns, an array of ≈70-nm-diameter dots was patterned at 200-nm pitch on the SiO_2 surface using an electron-beam lithography system (JEOL, JBX-6300FS), and very thin patterns (3-nm-thick titanium and 3-nm-thick gold) were deposited using the electron-beam evaporator.

Surface preparation and AFM imaging: Origami was imaged in tapping mode in solution (TAE buffer) using Olympus Biolever tips and an Asylum MFP-3D AFM. Protocols were slightly different for each surface used. For freshly cleaved mica, 2 μL of unpurified origami was deposited for 2–3 min and 100–200 μL of TAE buffer was added for imaging. For unpatterned gold surfaces, the gold was briefly cleaned in piranha solution (3:1 v/v concentrated sulfuric acid/30% hydrogen peroxide) and rinsed in DI water and ethanol. A UV ozone reactor (PR-100, UVP, Upland, CA) was also used for 10–20 min of additional cleaning. The micrometer-sized patterned gold surfaces were cleaned only by ozone cleaning and rinsing in DI water and ethanol. These surfaces were then placed in a 1 mM solution of 11-mercaptoundecanoic acid (MUA) in ethanol for 12+ h, after which they were rinsed in ethanol several times, dried with nitrogen, and attached to a glass slide for AFM

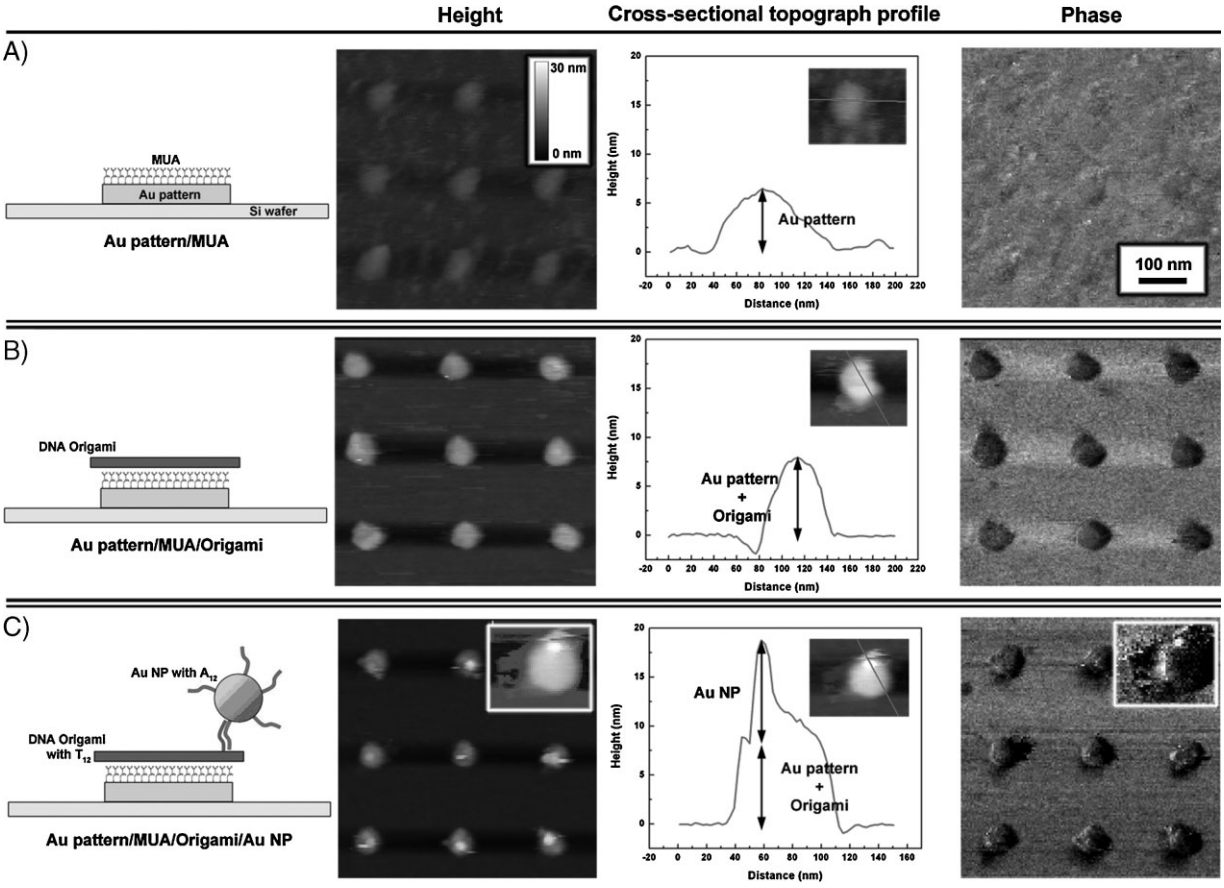

Figure 4. Delivery of individual DNA origami structures to 70-nm-diameter gold patterns (note: all images are taken at the same scale). A) Gold patterns functionalized with MUA exhibit ≈6-nm topography in height mode and minimal contrast in phase mode. B) The additional thickness of immobilized origami structures on the gold patterns produces the expected ≈2-nm increase observable in height-mode AFM. Significantly higher contrast can be observed in phase mode due to the large difference in material properties. C) Successful delivery of 10-nm-diameter gold nanoparticles onto an array of immobilized origami structures can be clearly observed in height mode, with the presence of nanoparticles indicated by the protruding features (bright dot) visible atop individual origami structures. The cross-sectional profile reveals the expected ≈18-nm topography. The rectangular outlines of the immobilized origami can also be observed in the phase mode.

imaging. Unpurified origami structures (3–5 μL) were deposited on the surface for 2–3 min and 100–200 μL of TAE buffer was added prior to imaging. For nanometer-sized gold patterns, the same protocol was used but before AFM imaging patterns were rinsed several times with 1× TAE buffer after the addition of origami structures (5 μL) and nanoparticles (5 μL), respectively, in order to eliminate physisorbed particles.

Keywords:
DNA · nanoparticles · origami · self-assembly · surface patterning

[1] H. Yan, S. H. Park, G. Finkelstein, J. H. Reif, T. H. LaBean, *Science* **2003**, *301*, 1882.
[2] N. C. Seeman, *Nature* **2003**, *421*, 427.
[3] P. W. K. Rothemund, *Nature* **2006**, *440*, 297.
[4] J. Sharma, R. Chhabra, C. S. Andersen, K. V. Gothelf, H. Yan, Y. Liu, *J. Am. Chem. Soc.* **2008**, *130*, 7820.
[5] D. H. J. Bunka, P. G. Stockley, *Nat. Rev.* **2006**, *4*, 588.
[6] A. D. Ellington, J. W. Szostak, *Nature* **1990**, *346*, 818.
[7] R. Chhabra, J. Sharma, Y. Ke, Y. Liu, S. Rinker, S. Lindsay, H. Yan, *J. Am. Chem. Soc.* **2007**, *129*, 10304.
[8] C. Lin, Y. Ke, Y. Liu, M. Mertig, J. Gu, H. Yan, *Angew. Chem. Int. Ed.* **2007**, *46*, 6089.
[9] A. Kuzyk, B. Yurke, J. J. Toppari, V. Linko, P. Torma, *Small* **2008**, *4*, 447.
[10] Y. Ke, S. Lindsay, Y. Chang, Y. Liu, H. Yan, *Science* **2008**, *319*, 180.
[11] D. A. Chernoff, in: *Proceedings Microscopy and Microanalysis*, Jones and Begell, New York **1995**.
[12] O. P. Behrend, L. Odoni, J. L. Loubet, N. A. Burnham, *Appl. Phys. Lett.* **1999**, *75*, 2551.
[13] R. Garcia, R. Magerle, R. Perez, *Nat. Mater.* **2007**, *6*, 405.
[14] M. Lysetska, A. Knoll, D. Boehringer, T. Hey, G. Krauss, G. Krausch, *Nucleic Acids Res.* **2002**, *30*, 2686.
[15] J. C. Love, L. A. Estroff, J. K. Kriebel, R. G. Nuzzo, G. M. Whitesides, *Chem. Rev.* **2005**, *105*, 1103.
[16] M. Bezanilla, S. Manne, D. E. Laney, Y. L. Lyubchenko, H. G. Hansma, *Langmuir* **1995**, *11*, 655.
[17] J. N. Israelachvili, in: *Intermolecular and Surface Forces*, Academic Press, London **1991**.
[18] P. D. Ashby, C. M. Lieber, *J. Am. Chem. Soc.* **2005**, *127*, 6814.
[19] J. J. Storhoff, R. Elghanian, R. C. Mucic, C. A. Mirkin, R. L. Letsinger, *J. Am. Chem. Soc.* **1998**, *120*, 1959.

Received: March 13, 2009
Published online: May 12, 2009

